Proceedings of the 17th Biennial Waste Processing Conference
ASME 1996

EFFECT OF AIR DISTRIBUTION ON SOLID FUEL BED COMBUSTION

Jing T. Kuo, Wu-Shung Hsu and Tau-Chi Yo
Dept. of Mechanical Engineering
National Taiwan University
Taipei, Taiwan
Rep. of China

ABSTRACT

One important aspect of refuse mass-burn combustion control is the manipulation of combustion air. Proper air manipulation is key to the achievement of good combustion efficiency and reduction of pollutant emissions. Experiments, using a small fix-grate laboratory furnace with cylindrical combustion chamber, were performed to investigate the influence of undergrate/sidewall air distribution on the combustion of beds of wood cubes. Wood cubes were used as a convenient laboratory surrogate of solid refuse. Specifically, for different bed configurations (e.g. bed height, bed voidage and bed fuel size, etc.), burning rates and combustion temperatures at different bed locations were measured under various air supply and distribution conditions.

One of the significant results of the experimental investigation is that combustion, with air injected from side walls and no undergrate air, provide the most efficient combustion. On the other hand, combustion with undergrate air achieves higher combustion rates but with higher CO emissions.

A simple one-dimensional model was constructed to derive correlations of combustion rate as functions of flue gas temperature and oxygen concentration. Despite the fact that the model is one dimensional and many detailed chemical and physical processes of combustion are not considered, comparisons of the model predictions and the experimental results indicate that the model is appropriate for quantitative evaluation of bed burning rates.

INTRODUCTION

Combustion of solid fuels on a fixed or moving grate is common to many combustion facilities ranging from coal burning combustors to solid waste incineration furnaces. In the combustion processes, air is introduced to the furnace from beneath the grate as well as from the over-bed region to achieve good combustion efficiency. The distribution of undergrate and overfire air is known to play an important role in the combustion control of organic emissions from municipal waste combustors(Kilgroe, et al., 1990). Manipulation of the undergrate air allows control of the combustion processes and burning rates. The overfire air, injected at high velocity through nozzles on furnace walls, can effect complete combustion by entrainment and by promoting turbulent mixing of off-gases and entrained solids from the fuel bed.

Good mixing is essential for efficient combustion and it is achieved by introducing the proper amounts of air at the proper locations. Practical design and operation guidelines, mostly based on decades of experiences in coal and wood burning, for combustion air control are generally dependent upon the furnace design and fuel characteristics. Due to the complexity of furnace geometry, variation in fuel properties, and associated thermal and chemical processes, theoretical analysis of solid fuel bed combustion are limited only to simplified situations. Recently, with advances in computational fluid dynamics, two-dimensional furnace flow and thermal analysis have been attempted by researchers to aid the design of combustion air nozzles(Ravichandran and Gouldin, 1992, and Bette, M, et al., 1994). Despite all these, fundamental understanding of the mechanisms of solid fuel bed combustion is still insufficient for establishing general guidelines of broad applicability on combustion air distribution design and control.

With the aim of gaining more fundamental knowledge of effects of air supply and distribution on solid fuel bed combustion processes, laboratory experiments were conducted to provide data as the basis for analyzing the physical and chemical processes of solid fuel bed combustion and

mathematical modeling. The solid material selected for combustion experiments was wood. Wood, by itself, is considered as an important form of biomass fuel, on the other hand, it is also a convenient surrogate of solid refuse for laboratory investigation. Wood combustion has been studied by researchers for many years(e.g. Dadkhah-Nikoo and Bushnell,1994; Kanury, 1994). In the recent work of Dadkhah-Nikoo and Bushnell(1994), investigating wood combustion in a bench scale wood furnace, the ratio of underfire air and overfire air, and the inject locations of overfire air are identified as two of the important factors in combustion processes.

Other factors which could influence the solid fuel bed combustion include the physical and chemical characteristics of the bed materials, the average size of the solids, the bed height, the bed voidage, and bed agitation. The prime interest of this study is to obtain combustion data as basis to analyze the solid fuel bed combustion processes for various solid fuel beds under different air supply conditions.

COMBUSTION MODEL

In theory, the combustion rate is proportional to the oxygen consumption rate as the air filtering through the fuel bed. The oxygen level in the product gases indicates the fraction of unused(or excess) air. Under steady state conditions, assuming the oxygen concentration is varying one-dimensionally through the fuel bed, it can be shown that the oxygen concentration profile, in terms of oxygen mole fraction X_{O2}, in the fuel bed is

$$\frac{X_{O_2}}{1-a_r X_{O_2}} = \frac{1}{a_1}\exp(-Ky^*) \qquad (1)$$

where K is a reaction rate constant which may be temperature dependent and limited by the rate of diffusion of oxygen to fuel surfaces. If the chemical reactions of the combustion processes are known, from mass balance consideration, the combustion air to fuel ratio is related to oxygen concentration in the product gases by (Kuo, 1994)

$$R_{af} = \frac{4.76g}{\left(1-a_1\dfrac{X_{O_2,b}}{1-a_r X_{O_2,b}}\right)} \qquad (2)$$

In Eqs. (1) and (2), a_1=4.76 - a_r where a_r is a numerical factor arising principally because of the change of gaseous moles in reaction, and g is the molar oxygen/fuel ratio of the combustion reaction. For example, if the chemical formula of the refuse is expressed as $C_aH_bO_c \cdot f(H_2O)$, the combustion reaction is

$$C_aH_bO_c \cdot f(H_2O) + gO_2 \rightarrow a(1-r_{co})CO_2 + ar_{co}CO + (b/2+f)H_2O \qquad (3)$$

where r_{co} is the factor introduced to achieve different degree of CO formation in the combustion reaction, and g is the oxygen-to-fuel mole ratio,

$$g = a\left(1-\frac{1}{2}r_{co}\right) + \frac{b}{4} - \frac{c}{2} \qquad (4)$$

For this reaction a_r is

$$a_r = 1 - \frac{1}{g}\left(a + \frac{b}{2} + f\right) \qquad (5)$$

From the fuel bed energy balance, assuming no heat losses, and with the oxygen concentration distribution described by Eq. (1), the gas temperature leaving the fuel bed is,
if $a_r \neq 0$,

$$T^* = 1 + \frac{q^*}{g}\ln\left[\left(1+\frac{a_r}{a_1}\right)\left(1-a_r X_{O_2,b}\right)\right]\frac{M_{fuel}}{M_{gas}} \qquad (6a)$$

And, if a_r=0,

$$T^* = 1 + \frac{q^*}{g}\left(\frac{1}{a_1} - \frac{X_{O_2,b}}{1-a_r X_{O_2,b}}\right)\frac{M_{fuel}}{M_{gas}} \qquad (6b)$$

Combining Eqs. (2) and (6a or b), by eliminating $X_{O2,b}$ between these two equations, implicitly, a correlation of air to fuel ratio as a function of temperature can be obtained.

TABLE 1. TEST CONDITIONS

Exp. No.	1	2	3	4	5	6	7	8
Bed Height(mm)	400	400	400	485	400	400	400	400
d_{eff}, Solid size(mm)†	29	29	29	25	30	35	40	51
a_{pv} mm^{-1}	0.105	0.105	0.105	0.103	0.134	0.101	0.078	0.057
Initial bed voidage, ε	0.49	0.49	0.49	0.58	0.33	0.42	0.48	0.51
Undergrate air N*l*‡ /min	240	300	200	200	-	-	-	-
Sidewall air N*l*/min	60	-	100	100	100 to 300	100 to 300	100 to 300	100 to 300
Sidewall air injection port location	g	-	c	c	a to g	a to g	a to g	a to g
Initial bed mass(kg)	5.0	5.0	5.0	5.0	6.5	5.8	5.1	4.8

† $d_{eff} = 6\frac{V_s}{A_s}$ V_s: volume , A_s: surface area

‡ N*l* Normal liter=gas volume of 1000 cm^3 at 25 °C and 1 atm

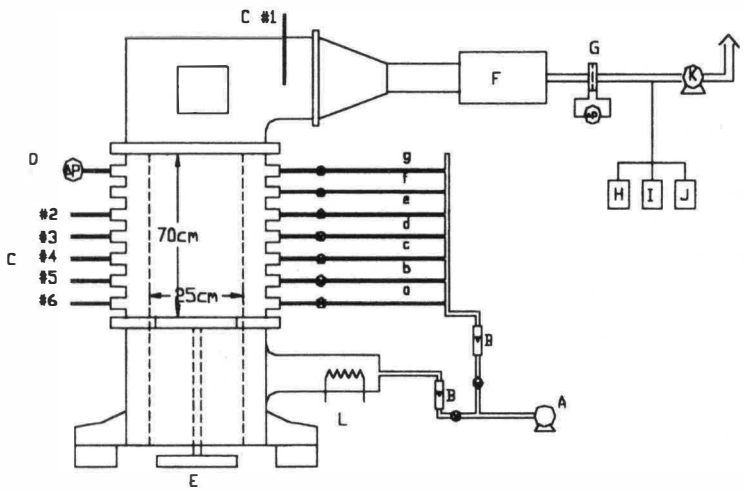

A : Air blower , 3Hp , 2.4m~3/min , 1500Aq

B : Rotameter 0~300Nl/min

C : K type thermocouple

D : Pressure gauge

E : Strain gauge load cell , 0~35kg

F : Flue gas cooling heat exchanger

G : Orifice flow meter

H,I,J : O2 , Co , Co2 analyzer

K : Draft fan , 1Hp , 10.7m~3/min , 360mmAq

L : Air heater

Fig. 1 EXPERIMENTAL FACILITIES

EXPERIMENTAL FACILITIES

The combustion system used in this work is described in Figure 1. Basically, it consists of a combustion furnace, an air blower, a flue gas cooling heat exchanger, an orifice flow meter and a draft fan.

The experimental furnace is a cylindrical combustion chamber, with 250 mm inside diameter and 75mm thick wall lined with high temperature castable refractory. The grate is movable vertically and connected to a strain-gauge load cell in order to measure the bed mass lost in combustion. The internal height of the combustion chamber is 700 mm.

A total of six K-type thermocouple temperature sensors are installed at various locations above the grate. Thermocouple No. 1 is located in the upper portion of the furnace from where the combustion products are ducted to the flue gas cooler. The other 5 thermocouples are spaced 90mm apart and the lowest one is located at a distance of 90mm above the grate. For each test, flue gas samples including O_2, CO_2 and CO were monitored and recorded continuously down stream of the flue gas cooling heat exchanger.

TEST CONDITIONS AND PROCEDURES

Wood samples for the experiments were prepared in cubical or rectangular shape cut from wood bars of 25mm×25mm cross section with effective sizes, d_{eff}, ranging from 25 mm to 50 mm . Based on the results of laboratory chemical analysis, the chemical formula of the wood sample can be approximately expressed by $C_6H_{10}O_7 \cdot 8H_2O$. The ash content is 2.56%. Table 1 summarizes the test conditions of the combustion experiments. Variations of test parameters are mainly in the distribution of air supply and fuel particle size. Experiments No. 1 to 4 were a group of tests performed under fixed rate of total air supply with different air distribution conditions. Experiments No. 5 to 8 were conducted with no undergrate air, all the combustion air was injected through the side wall. The combustion air is introduced to the furnace both from beneath the grate and through tiny air holes along the side wall. The locations of wall air injection can be positioned below or above the bed top level. For experiments No.5 to 8, the air flow rate was increased every 10 min. beginning at 100 N*l*/min and ending at 300 N*l*/min. Although no undergrate air was used in experiments No. 5 to 8, a portion of the air was injected "underfire", thus the overfire/underfire ratio was changing during the course of experiment.

For each experiment, the fuel bed was ignited manually beginning from the top of the bed. In each combustion test, the temperature histories of each thermocouple were recorded continuously at 5 sec. interval. The furnace grate is connected underneath to a load cell outside of the furnace to weigh the mass of the bed. The coad cell was calibrated to correct the effects of undergrate air drag and other frictions. The air drag could cause a reduction of weight measurement up to 2.5% at the highest air flow (300 N*l*/min) condition.

The test conditions of the experiments, in terms of air flux(based on grate area) and grate combustion rate(mass burned per unit grate area per unit time), are near the lower end of that of the commercial facilities. The highest air flux used in this work was 0.1 $Nm^3/m^2/sec$, while the commercial incineraor may operated in the range of 0.1 to 0.3 $Nm^3/m^2/sec$. For commercial facilities, the grate combustion rates are generally in the range of 100 to 150 $kg/h/m^2$ for fixed grate furnaces and 200 to 500 $kg/h/m^2$ for mechanical grates. In this work, the grate combustion rates were below 250 $kg/h/m^2$.

RESULTS AND DISCUSSIONS

Combustion Temperature

Figure 2 shows the typical temperature history(citing experiment No. 1 as an example) recorded by each thermocouple at different locations. Generally, thermocouple #6, located at the very bottom near the grate, had the highest temperature reading which was around 1100 ^oC. For experiment No. 1, as shown in Figure 2, toward the end of the burning processes(around t=40min), all the thermocouples showed an increase in temperature. This phenomenon was also observed in experiment No. 2(see Figure 3). Presumably, this signifies that at the end of the experiment all the temperature sensors were exposed to the radiation of the flame. For experiments No. 3 and 4, this type of end-of-experiment temperature rise phenomenon(not shown in this paper) is not obvious. The combustion temperature achieved at the furnace exit is generally higher for tests with only sidewall air supply, namely experiments No. 5 to 8, than for those with undergrate air supply.

Temperature measured by thermocouple #2 which is located nearest to the top of the combustion chamber, is selected to represent the combustion gas temperature. Figure 3 shows the temperature history curves of thermocouple #2 for experiments No. 1 to 4. The patterns of the curves for experiments No. 1 and 2 are distinctly different than those of experiments No. 3 and 4. Injection of combustion air from the sidewall below the bed top level tends to smooth out the temperature variations and produces higher combustion temperature. Figure 4 is the gas temperature history for experiments No. 5 to 8. The results indicate that fuel beds with higher initial void fractions have lower combustion temperature.

Combustion temperature and oxygen level in the product gases play important roles in combustion control, and variations in gas temperature and oxygen level in the product gases are often related. Figure 5 shows the correlation between gas temperature and oxygen concentration in the product gases. It can be seen from Figure 5, seemingly, there are two groups of data, one group consists of test data mainly from the tests without undergrate air supply and the other group consists entirely of test data obtained from experiments with undergrate air supply. The curves in Figure 5 are the predications of Eq.(6), assuming the carbon in fuel is either reacted to CO_2 or to CO. The data of those tests with undergrate air(Exp. No. 1 to 4) are better fitted by the carbon-to-CO curve. This is in agreement with the emission measurements that the CO emission is higher

for those tests with undergrate air than those without.

Comparisons of temperature data of experiments No. 3 and 4, respectively, with those of experiments 5 to 8 are shown in Figures 6 and 7. Figure 6 shows that the combustion temperatures achieved in experiment No. 3, with undergrate air supply, were generally lower than those tests with purely wall air injection. In Figure 7, part of the data points of experiment No. 4 are well mingled with test data of experiments 5 to 8, they are associated with the temperature rising stage of the combustion processes. At the same oxygen level, the temperatures in the beginning stage of the combustion are generally higher than those at the trailing stage of the combustion. This may indicate that the combustion chemistry and the thermal energy transfer conditions were changing during the course of the experiment.

Excess O_2

Gas samples were taken at a location down stream of the flue gas cooler. As shown in Figure 8, for experiments No.1 to 4, the oxygen levels are mostly under 5%. For experiments No. 3 and 4, the oxygen concentration showed an increase when the bed level dropped below the sidewall air injection port.

Figure 9 shows the measured oxygen concentration in relation to air flows for tests with only sidewall air supply. Combustion with sidewall air flows only, the amount of excess O_2 is decreasing with increasing air flow rate. The oxygen level for a bed with lower initial void fraction is lower than a bed with higher initial void fraction. For the same air flow, a lower oxygen concentration at the bed top means higher oxygen consumption and higher burning rate, and as a result, higher combustion temperature. This is in agreement with the trends of combustion temperature and combustion rate measurements.

One the whole, the oxygen levels in the off-gases of tests with only sidewall air injection, were generally higher than those of the tests with undergrate air supply.

Combustion Rates

The combustion rates are calculated based on the bed weight losses measured by the load cell. The grate burning rate is defined by

$$\omega = \frac{M(t) - M(t+\Delta t)}{A_{bed} \cdot \Delta t} \qquad (7)$$

This expression essentially represents the derivative of the bed weight loss curve.

Figure 10 shows the bed weight loss curves of the combustion experiments. Figure 11 shows the time variations of grate burning rates estimateded by using Eq. (7). Examining the slopes of mass loss curves in Figure 10, one can see that the burning rates are increasing with increasing undergrate air flow rates. For experiments No. 3 and 4, the sidewall air flows were initially introduced to the furnace beneath the top of the bed. When the bed top level dropped below the sidewall air injection port, the combustion changed to lower rates due to reduction in bed air supply.

For experiments No. 1 and 2, on the average, the combustion rates incresed slightly in the later stage of the burning processes. A possible cause for this could be related to the redistribution of bed materials when the bed started to crumble. The influence of bed particle size and voidage on combustion rate is also evident from the test data. For example, in experiment No. 3, with a fuel bed of higher initial a_{pv}(solid surface area per unit bed volume), the burning rates were higher than that of the experiment No. 4 in the initial stage of the combustion process. In the later stage of the burning processes, the burning rates of experiment No. 4 became higher. A fuel bed which is initially more loosely packed, may be easier to crumble during combustion than a more tightly packed bed. This may explain that , for experimant No. 4, toward the later stage of the combustion processes, the combustion rates became higher when the partially burned solids shrunk in size and began to filling in the gaps of the lower portion of the bed. For experiments No. 5 to 8, which had only sidewall air flows, the combustion rates also showed a positive correlation with the air flow rates. Figure 12 shows the curves of combustion rates versus air flow rates for the experiments with only sidewall air flows. For the same air flow, a bed with lower voidage, or higher solids surface area, can achieve higher combustion rates. On the other hand, comparing Figures 11 and 12, one may conclude that higher combustion rates can be achieved with undergrate air supply.

The data of combustion rate versus temperature for experiments No. 3 and 4 in comparison with experiments No. 5 to 8 are shown respectively in Figures 13 and 14. The combustion rates for experiments No. 5 to 8 are fitted quite well with combustion temperature based on the Arrhenius type of correlation. The solid curves in Figures 13 and 14 are represented by the following equation.

$$\omega = 45.17 \exp\left(-\frac{6777.13}{RT}\right) \qquad (8)$$

The unit of ω is in $g/cm^2 \cdot sec$ and R is the gas constant in $kcal/kgmole \cdot {}^\circ K$. The Arrhenius type of combustion rate dependence on temperature is not obvious for experiments No. 1 and 2. For experiments No. 3 and 4, the test data indicate that for the same temperature, the combustion rates are higher in the temperature increasing stage (or the beginning stage) of the combustion processes. The may reflect that the combustion chemistry is changing during the course of the combustion processes. The dashed lines in Figures 13 and 14, are curvefit to

TABLE 2 FLAME SPREADING VELOCITY (cm/min)

Thermocouple	#2 to #3	#3 to #4	#4 to #5	#5 to #6
Exp. 1	1.8	1.8	1.5	2.2
Exp. 2	3.0	1.8	2.2	1.78
Exp. 3	2.0	2.0	1.1	1.47
Exp. 4	2.25	2.0	1.57	1.3

those up-trend data points.

The total air flow rates for experiments No. 1 to 4 are the same, except with different air supply distribution patterns. Figure 15 shows the combustion rates as a function of combustion temperature for experiments No. 1 to 4 in comparison with those test data of experiments No. 5 to 8 at the same air flow rate . The curves in Figure 15 are predications of Eqs. (2) and (6) based on the experimental air supply rate of 300 Nl/min. The data shown in Figure 16 describe the relationship between combustion rates and oxygen concentrations. The curves in Figure 16, which bound most of the test data, are predications of Eq. (2), assuming the chemical formula of the bed materials is $C_{10}H_{16}O_7 \cdot 8H_2O$, for two different combustion chemical reactions, carbon-to-CO_2 and carbon-to-CO.

Air to Fuel Ratio

Air to fuel ratio is defined as the ratio of total air flow rate to fuel bed gasification rate. Based on the combustion rate measurements, air to fuel ratio can be calculated. Figure 17 is the plot of measured air/fuel ratio versus oxygen level in the combustion product gases. The curves shown in Figure 17 are predictions of Eq. (2), assuming the chemical formula of the bed materials is $C_{10}H_{16}O_7 \cdot 8H_2O$.

Figure 18 shows the data of gas temperature as a function of air to fuel ratio. The curves in Figure 18 are predictions of Eqs. (2) and (6), for the extreme conditions of either all the carbon is converted to carbon dioxide or to carbon monoxide. Again, practically, all the test data are bounded by the theoretical curves.

Flame Spreading

The spreading of the combustion processes can be estimated based on the responses of the thermocouples. The combustion spreading velocity shown in Table 2 is calculated based on the time required for each thermocouple to reach 200 ^{o}C temperature reading. The distance between each thermocouple (#2 to #6) is 90 mm. For experiments No. 5 to 8, the temperature histories of thermocouples #3 to #6 were not recorded, thus the flame spreading behaviors for these tests are unavailable.

CO_2 Concentration

For all the tests, the sum of O_2 and CO_2 concentrations stays constant around 16%. Figure 19 shows the correlation between $CO_2$and O_2 for experiments No. 5 to 8.

CO Emission

CO emission is dramatically lower, below 50 ppm, for those tests with sidewall air injection only. In those combustion experiments with undergrate air supply, the CO emission levels recorded could be higher than 800 ppm at extremely low oxygen concentrations. Injection of sidewall air was helpful in reducing the CO level, but not significantly. In experiments No. 3 and 4, all the sidewall air injection ports were initially below the bed top level, when the bed level fell below the air injection port, a roughly 12% drop in CO emission was observed. To further reduce CO emission, a higher portion of overfire air injection may be needed. Figures 20 and 21 display the CO concentration as a function of excess O_2. One of the major differences between Figure 20 and Figure 21, is that the test data of experiments No. 1 to 4 indicate that CO emission is decreasing with increasing oxygen concentration, while the test data of experiments No. 5 to 8 show the opposite trend. For tests with sidewall air flow only, both the oxygen and CO concentrations in the off-gases were increasing with decreasing air flow rates. In this case, the extra aomunt of oxygen, instead of promoting the completion of combustion reactions as the overfire air jets would usually do, may actually had a quenching effect on the combustion reactions which kept the CO at high levels.

CONCLUSIONS

One of the major influences of air distribution on solid bed combustion is in combustion rate. For the same amount of total air flow, the combustion rates are increasing with increasing undergrate air flow rates. Injection of air to the fuel bed from the side wall is helpful in promoting fuel-air mixing and achieveing more complete combustion, but this tends to lower the combustion rates.

The test results indicate that combustion temperature is more uniform when air is injected from the side wall. This shows that fluctuations in combustion temperature, which is typical in batch combustion of solid fuel bed can be smoothed by proper stoking to promote better mixing.

Although the test data show that combustion rate and air to

fuel ratio are directly related to combustion temperature, correlating the combustion rate with temperature based on the frequently used Arrhenius type of temperature dependence is not generally applicable. The pattern of air supply and distribution has a profound influence on the chemistry of solid fuel bed combustion. The correlation of combustion rate with combustion temperature given by Eqs. (2) and (6), in comparison with the test data, is qualitatively correct in predicting the trend of combustion rate-temperature relationship, and quantitatively, the predictions cover the same range as that of the test data, thus, it could provide a theoretical means of estimating the combustion rates based on temperature measurements.

Combustion rate is related to the fuel bed void fraction. For the same air flow, a higher burning rate can be achieved with a more tightly packed bed.

Flue gas oxygen content is an important parameter in combustion emission monitoring and control. In solid fuel bed combustion, with a given air flow, the oxygen level in the exhaust gases reflects the variations in combustion rates. Test data show that higher burning rates are associated with lower oxygen levels in the exhaust gases. The experimental data of combustion rate and air to fuel ratio versus oxygen concentration are well represented by Eq. (2).

Flue gas oxygen content and combustion temperature are also related, the trend predicted by Eq. (6) is in good agreement with the test data.

CO emission levels, when air is injected through the sidewall nozzles, can be significantly lower than combustion with undergrate air. CO emission is related to flue gas oxygen content in different ways depending upon the air introduction method. When undergrate air is used, CO emission is decreasing with increasing oxygen concentration. On the other hand, when air is injected through side wall which produces better mixing, CO emission is increasing even with increasing exhaust gas oxygen content.

ACKNOWLEDGEMENT

This work was partially funded by the ROC National Sciences Council, No. NSC 84-2211-E-002-002.

REFERENCES

Bette, M., et al., 1994, "The Achievement of "Good Combustion" by Improvement of Secondary Air Injection at the Montgomery County Waste to Energy Facility," ASME 16th Biennial National Waste Processing Conference Proceedings, pp. 163-170.

Dadkhah-Nikoo, A., Bushnell, D. J., 1994, "An Experimental Investigation of Wood Combustion," ASME J. of Energy Resources Technology, Vol. 116, pp.186-193.

Kanury, A. M., 1994, "Combustion Characteristics of Biomass Fuels," Combust. Sci. and Tech., Vol. 97, pp. 469-491.

Kilgroe, J. D., et al., 1990, "Combustion Control of Organic Emissions from Municipal Waste Combustors," Vol. 74, pp. 223-244.

Kuo, J. T., 1994,"Estimation of Burning Rates in Solid Waste Combustion Furnace," ASME 16th Biennial National Waste Processing Conference Proceedings, pp. 177-183.

Ravichandran, M., Gouldin, F. C., 1992, "Numerical Simulation of Incinerator Overfire Mixing," Combust. Sci. and Tech., Vol. 85, pp. 165-185.

NOMENCLATURES

A_{bed} Bed area

A_s Solids surface area

a Number of carbon atom in fuel chemical formula

a_l & a_r Numerical factors defined in Eqs. (1) and (2)

b Number of hydrogen atom in fuel chemical formula

C_{pg} Specific heat of the combustion products

c Number of oxygen atom in fuel chemical formula

d_{eff} Effective solid size, $6V_s/A_s$

f Number of H_2O in fuel chemical formula

g Stoichiometric oxygen to fuel mole ratio, Eq. (2)

H Fuel bed height

K Reaction constant, Eq. (1)

M Mass of the fuel bed

M_{fuel} Molecular weight of fuel

M_{gas} Molecular weight of combustion product gas mixture

q Heat of combustion

$q^*=q/C_{pg}T_o$ Dimensionless heat of combustion

R Gas constant, kcal/kgmole ^oK

R_{af} Air to fuel mole ratio

r_{CO} Fraction of carbon converted to carbon monoxide

T Temperature

T_o Reference temperature , 298 °K

$T^*=T/T_o$ Dimensionless temperature

t Time

V_s Solids volume

X_{O2} Mole fraction of oxygen in the gas products

$X_{O2,b}$ Mole fraction of oxygen in the gas products at the top of the fuel bed

$y^*=y/H$ Dimensionless bed height

ε Bed void fraction

ω Combustion rate $g/cm^2 \cdot sec$

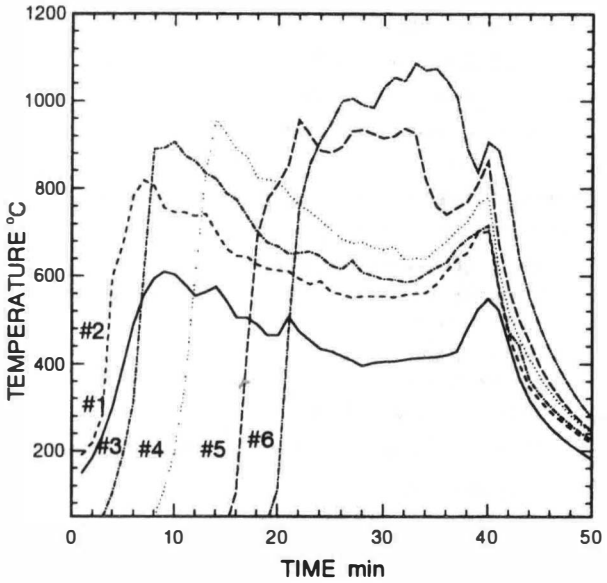

FIG. 2 TEMPERATURE HISTORY OF THERMOCOUPLE SENSORS(EXP. NO. 1)

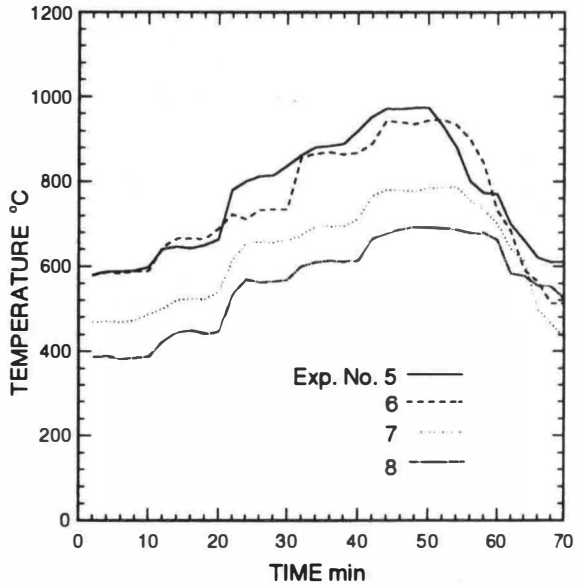

FIG. 4 TEMPERATURE HISTORY OF THERMOCOUPLE #2 NEAR THE TOP OF THE COMBUSTION CHAMBER

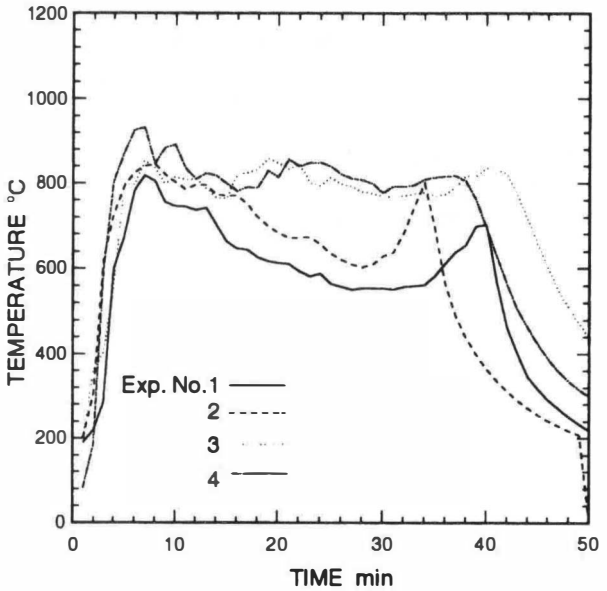

FIG. 3 TEMPERATURE HISTORY OF THERMOCOUPLE(#2) NEAR THE TOP OF THE COMBUSTION CHAMBER

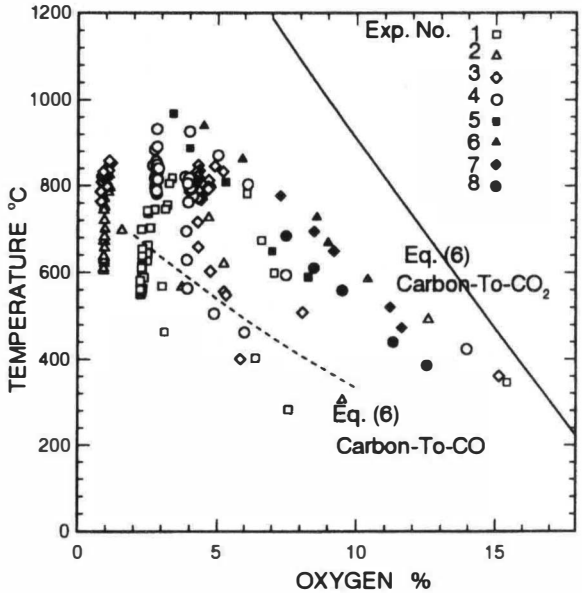

FIG. 5 COMBUSTION TEMPERATURE VERSUS OXYGEN CONTENT OF COMBUSTION PRODUCTS

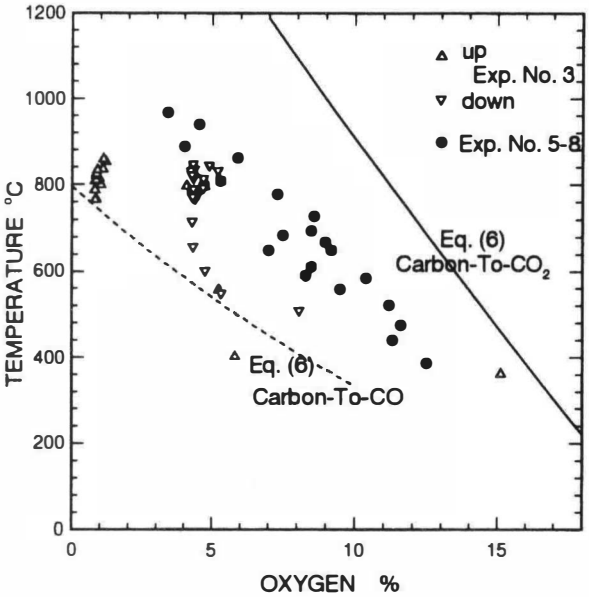

FIG. 6 TEMPERATURE AS FUNCTION OF OXYGEN CONTENT OF COMBUSTION PRODUCTS

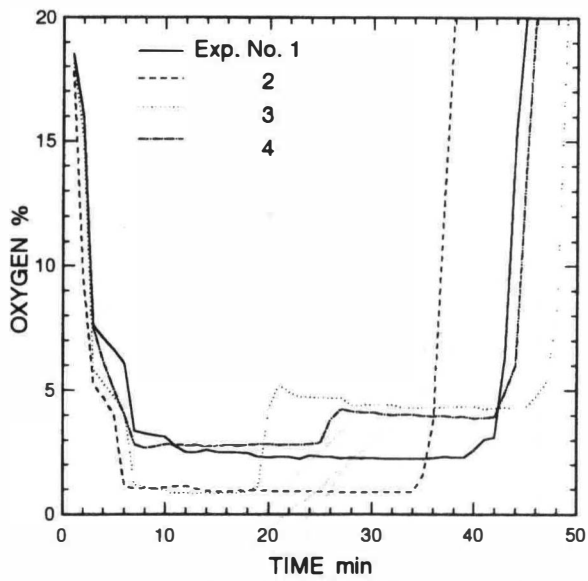

FIG. 8 TIME HISTORY OF OXYGEN CONTENT OF COMBUSTION PRODUCTS

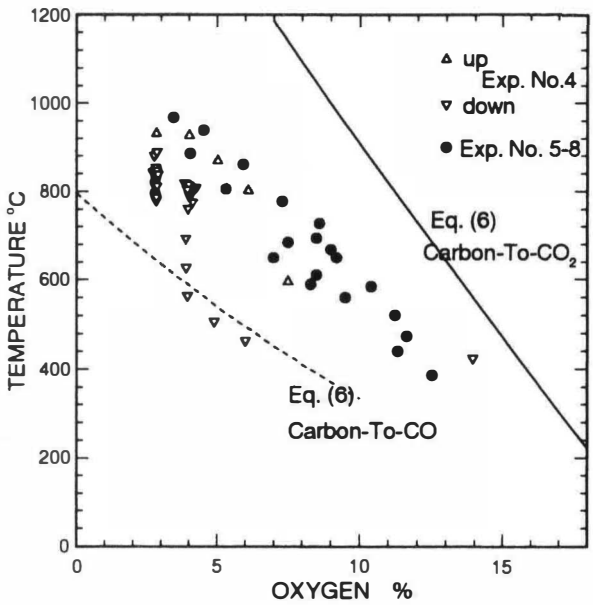

FIG. 7 TEMPERATURE AS FUNCTION OF OXYGEN CONTENT OF COMBUSTION PRODUCTS

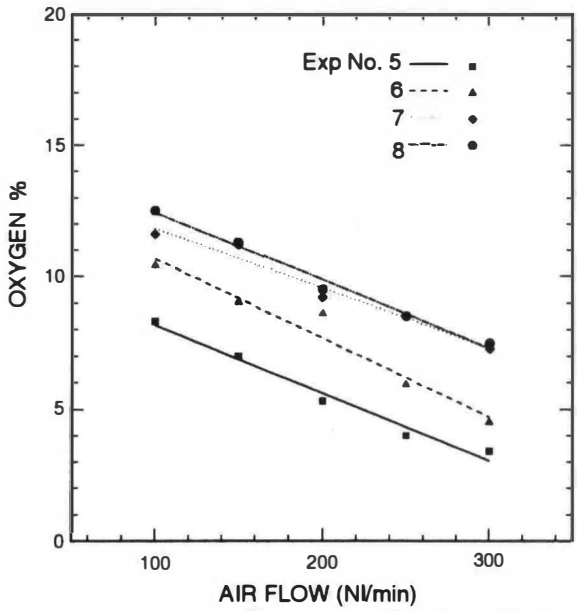

FIG. 9 OXYGEN CONTENT OF COMBUSTION PRODUCTS AS FUNCTION OF AIR FLOW

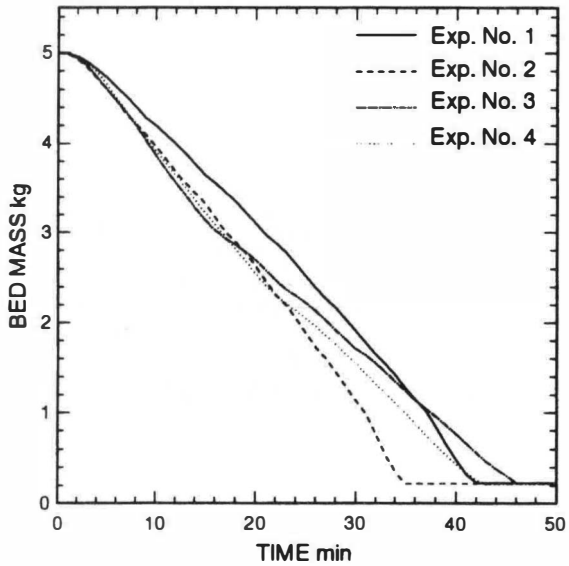

FIG. 10 BED MASS LOSS HISTORY

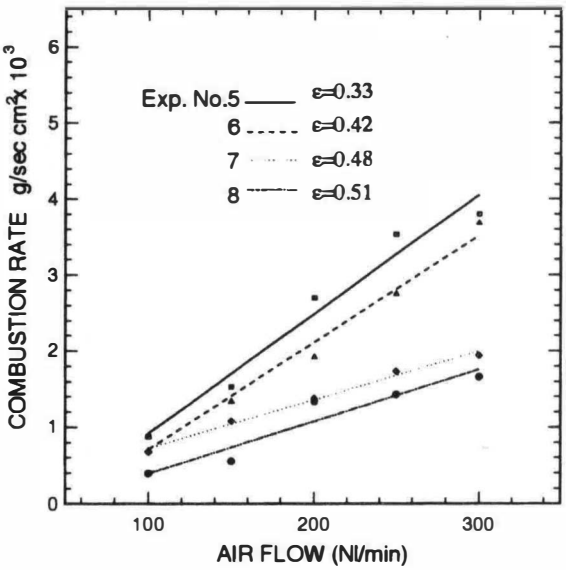

FIG. 12 COMBUSTION RATE AS FUNCTION OF AIR FLOW

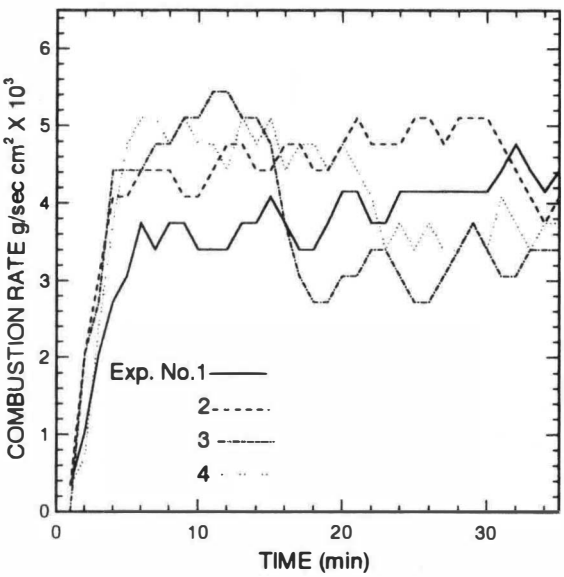

FIG. 11 TIME VARIATION OF COMBUSTION RATES

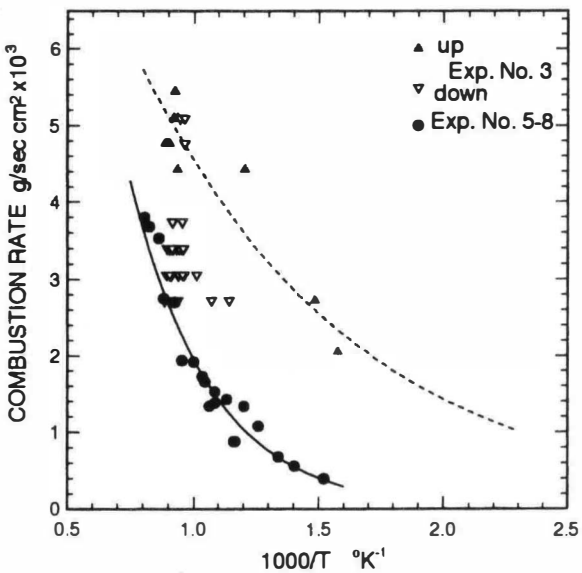

FIG. 13 COMBUSTION RATE VERSUS COMBUSTION TEMPERATURE

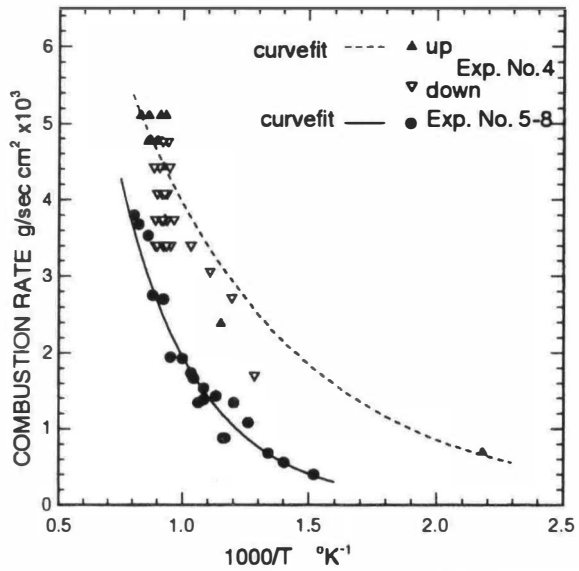

FIG. 14 COMBUSTION RATE VERSUS GAS TEMPERATURE

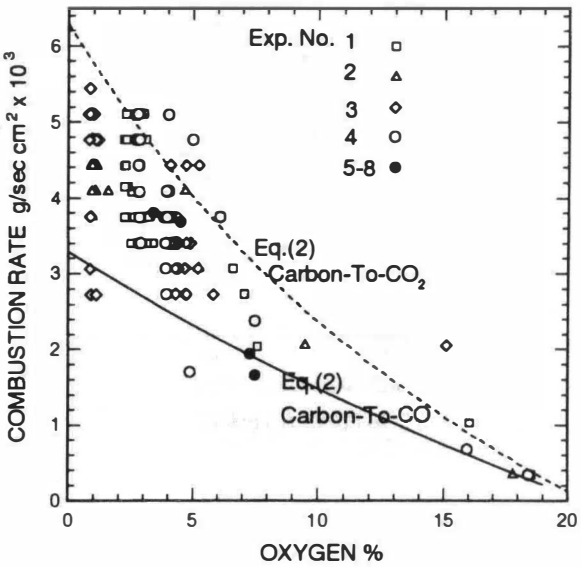

FIG. 16 COMBUSTION RATE VERSUS OXYGEN CONTENT COMBUSTION PRODUCTS

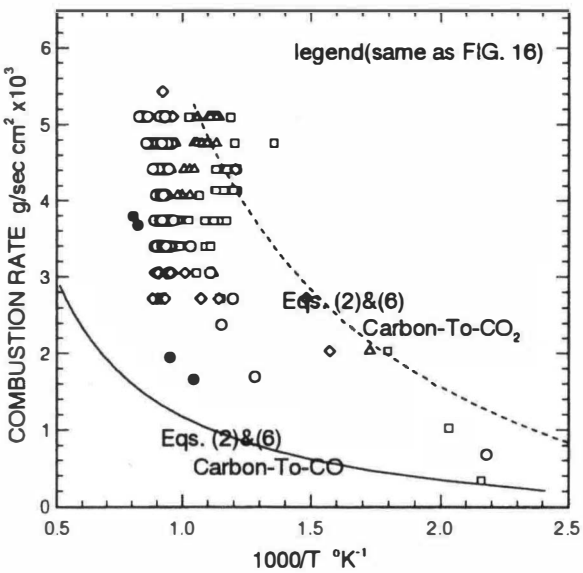

FIG. 15 COMBUSTION RATE VS. GAS TEMPERATURE

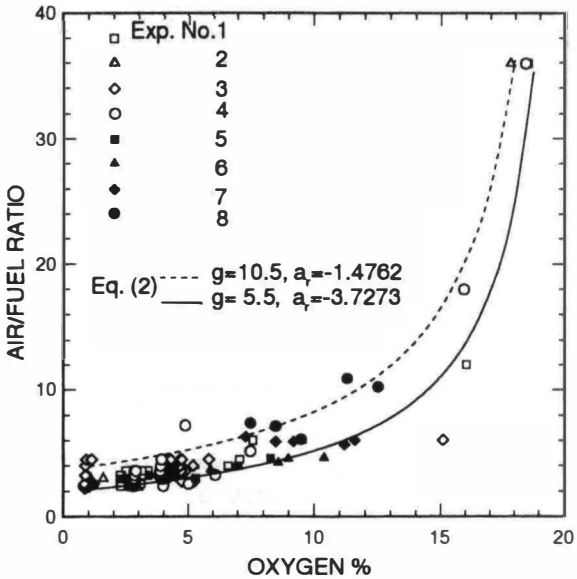

FIG. 17 AIR TO FUEL RATIO VS. FLUE GAS OXYGEN CONTENT

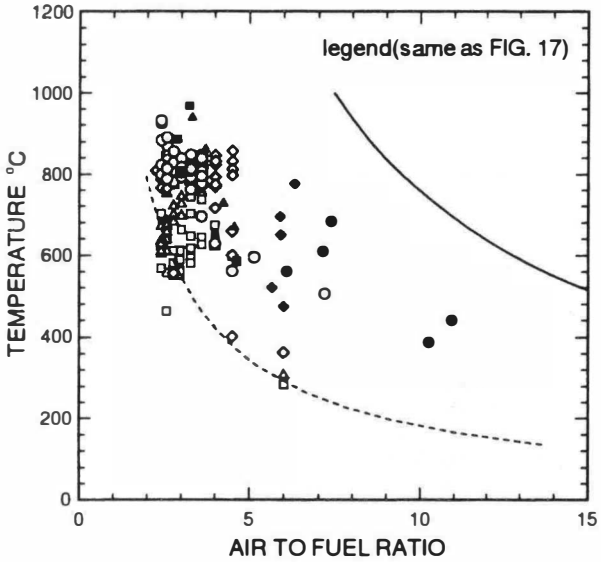

FIG. 18 GAS TEMPERATURE AS FUNCTION OF AIR TO FUEL RATIO

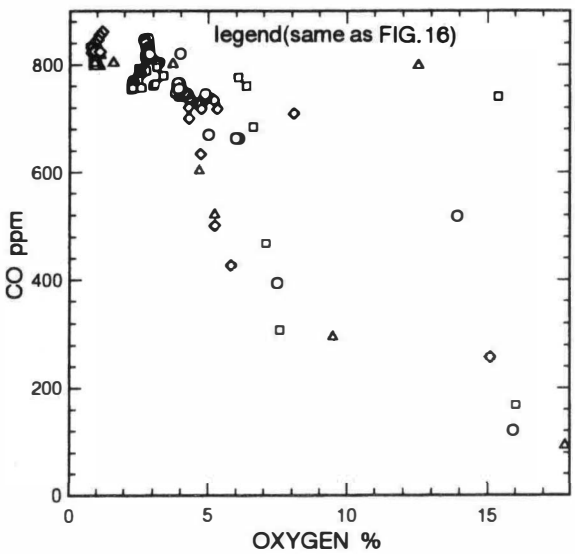

FIG. 20 CO EMISSION VERSUS OXYGEN CONTENT OF COMBUSTION PRODUCTS

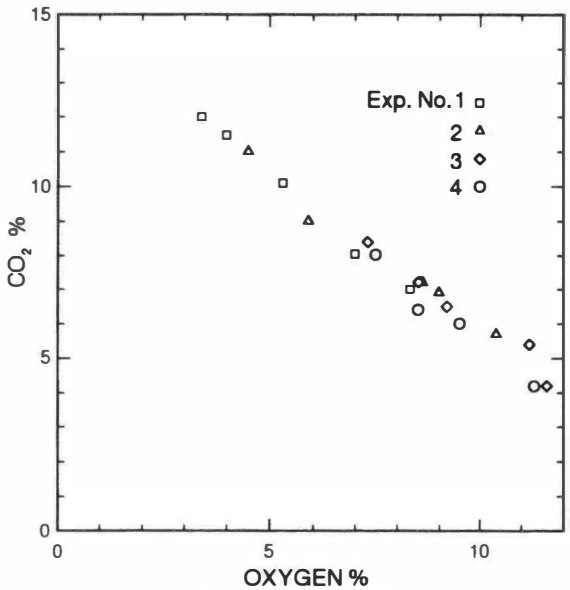

FIG. 19 CARBON DIOXIDE AND OXYGEN CONTENTS OF COMBUSTION PRODUCTS

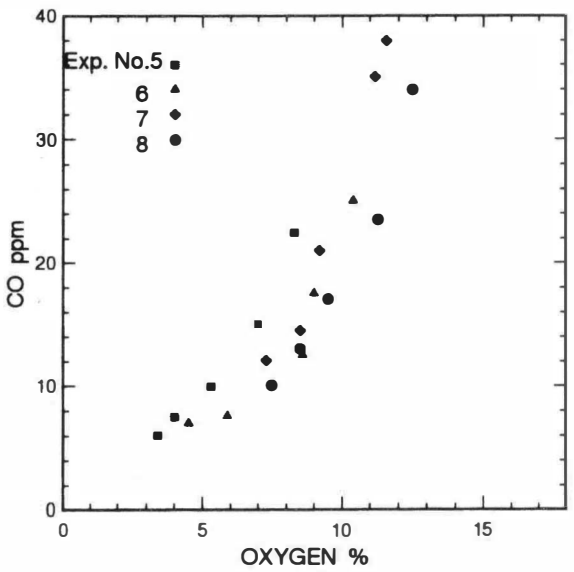

FIG. 21 CO EMISSION VERSUS OXYGEN CONTENT OF COMBUSTION PRODUCTS